Controlling the piezoelectric properties in bulk BiFeO$_3$-PbTiO$_3$-Li$_{0.5}$Bi$_{0.5}$TiO$_3$ ceramic by quenching and annealing

Tuluk, Anton; van der Zwaag, Sybrand

Important note
To cite this publication, please use the final published version (if applicable).
Please check the document version above.

Controlling the piezoelectric properties in bulk $BiFeO_3$–$PbTiO_3$–$Li_{0.5}Bi_{0.5}TiO_3$ ceramic by quenching and annealing

Anton Tuluk ✉ iD ; Sybrand van der Zwaag iD

Check for updates

View Online   Export Citation   CrossMark

Articles You May Be Interested In

Antiferroelectric orthorhombic *P*-to-*R* phase transition induced exotic electrocaloric effect in $NaNbO_3$-based lead-free ceramics

Appl. Phys. Lett. (March 2023)

Tuning piezoproperties of $BiFeO_3$ ceramic by cobalt and titanium dual doping

J. Appl. Phys. (June 2022)

Synthesis and Dielectric Study of NBT- BSN: a Lead Free Relaxor Materials

AIP Conference Proceedings (November 2011)

Anton Tuluk[a]) 🆔 and Sybrand van der Zwaag 🆔

AFFILIATIONS

Novel Aerospace Materials (NovAM), Faculty of Aerospace Engineering, Delft University of Technology, Kluyverweg 1, Delft, the Netherlands

[a])Author to whom correspondence should be addressed: A.Tuluk-1@tudelft.nl

ABSTRACT

In the present work, we study the effect of quenching and annealing on the ferroelectric and piezoelectric properties at room temperature and elevated temperatures of a new ternary BiFeO₃-PbTiO₃-Li₀.₅Bi₀.₅TiO₃ bulk piezo ceramic. While sacrificing part of the maximally obtainable piezoelectric constant value, using an optimal heat treatment, a quasi-stable value for the piezoelectric constant of 65 pC/N was obtained irrespective of the annealing temperature. All experimental results point to the direction of unusual defect behavior in this novel ternary system leading to a well-defined metastable state. The quenching and annealing process are completely reversible and can be used in combination with additional chemical modifications to tailor the properties of this new high-temperature piezoelectric ceramic to the intended use conditions.

I. INTRODUCTION

Electro-mechanical interactions between charged point defects and domain walls (DWs) play a key role in controlling the functional properties of bulk and thin-film ferroelectrics. Since the discovery of the presence and role of conducting domain walls in thin films of bismuth ferrite, it has been suggested that local conductivity increases with the presence of charged point defects.[1] Various types of defects have been proposed to maximize the effect, including oxygen vacancies, bismuth vacancies, holes, and electrons, highlighting the key role of defect chemistry and hence the material preparation processes (such as annealing temperature and cooling rate, as well as annealing atmosphere).[2,3] In previous studies on BiFeO₃ (BFO) thermally treated in air, it was shown that, in this material, the dominant defects at the domain walls are electron holes and bismuth vacancies. A reasonable assumption is that accumulated defects will lead to DW pinning effects affecting DW dynamics, such as displacements over short distances under the action of an applied electric field. It is possible that this mechanism will differ from that in prototype ferroelectrics, such as acceptor-doped hard Pb(Zr,Ti)O₃

(PZT) and BaTiO₃, in which strong attachment of DW is controlled by the acceptor–oxygen–vacancy defect complexes.[4–6] In addition to the type of defects, the pinning of DW is highly dependent on the spatial distribution of the defects.[7,8] Lacking evidence at the atomic level, macroscopic data on polarization switching in hard ferroelectrics based on PZT[9] and BiFeO₃[10] suggest that the degree of defect ordering can be controlled by the cooling rate from the high temperature annealing stage. It was proposed that quenching (i.e., fast cooling) the sample from a temperature above the Curie temperature (T_C) maintains the high temperature disordered state of the defects, while slow cooling promotes ordering of defects. This hypothesis is confirmed by a number of works on quenching of BiFeO₃-based piezoceramic,[11,12] which show an increase in piezoelectric properties and a decrease in the coercive field in bulk samples after quenching from above the Curie temperature.

Quenching in itself is a classic tool for constructing phase diagrams,[13] in addition to being widely used in heat treatment in the production of ferrous sheet metal and machined components and is used to tailor the general and local hardness, respectively.[14,15] For non-transforming metals and non-metallic ceramic and

polymeric materials, quenching is mainly used to retain the high temperature phase and to prevent undesirable phases from forming during cooling. Quenching is not widely used as a treatment option to control ferroelectric or piezoelectric properties of piezo ceramics, where property optimization is done more commonly via chemical modifications. The preference for chemical modification route is primarily due to the problems related to thermally initiated stresses leading to microcracks and failure of quenched ceramics.[16,17] Despite the obvious disadvantages, the quenching method, apart from being cheap and versatile, could be a promising tool for tailoring electromechanical properties and phase transitions in various ferroelectric and related materials. A recent work demonstrated that quenching from high sintering temperatures is beneficial in significantly increasing the thermal depolarization temperature in $Na_{0.5}Bi_{0.5}TiO_3$.[17] In earlier studies on BFO ceramics, the quenching method was used for two different reasons. The first is to effectively avoid an unstable region in the phase diagram. Quenching has been found to be a valuable technique to minimize the formation of secondary phases rich in Bi and Fe, which are commonly observed in BFO bulk ceramics synthesized via conventional processing.[18–20] The second reason relates to the behavior of charged point defects, in particular in relation to domain wall pinning, in which quenching was used to tune the distribution of defects.[21] The results showed the reason for the hardening behavior of BFO, which made it possible to truly reveal the influence of point defects on the switching properties of BFO and to provide insight even on the atomistic details of domain walls.[22] This hardening or softening behavior is crucial to tailor the piezo ceramic to the intended use. Hard piezoelectric materials can withstand high electrical and mechanical stresses, and their properties remain almost unchanged under these conditions. They are mainly used in high-power acoustics. The advantages of hard piezo materials are their moderate dielectric constant, large piezoelectric coupling factor, high mechanical quality, and good stability under high mechanical load and large working field strength. Soft piezoelectric refers to a type of ferroelectric piezoelectric ceramic with high mobility of the dipole and ferroelectric domains, which indicates easy low field polarization and depolarization characteristics. Soft piezo ceramics are generally used in piezoelectric actuators and sensors due to their high sensitivity and easy processing. Ceramics which can be processed into either hard or soft piezoceramics depending on the processing are of particular interest.

Quenching also has provided a new paradigm for improving the piezoelectric properties of BFO-based systems. As an example, the piezoelectric charge constant of $BiFeO_3–BaTiO_3$-based (BFO-BT) ceramics is significantly enhanced by the quenching process compared to the non-quenched state (commonly referred to furnace cooling, slow cooling, as-sintered).[17,23] Therefore, a quenching process is found to be one of the successful methods to improve piezoelectricity in BFO-based systems, and this has led to further research on the effect of quenching processes, such as quenching temperature and cooling rate.

There is a wide variety of BFO-based systems, but it is well known that systems which form a solid solution at or near the morphotropic phase boundary (MPB) region,[24] generally have the best properties including the highest piezoelectric constants. One such system is the MPB composition in $BiFeO_3–PbTiO_3$ which offers a high Curie temperature ($T_c = 635\,°C$), but which is hard to pole without cracking due to the large spontaneous strain. Furthermore, their p-type conductivity is too high for high temperature operation. On the other hand, other tetragonal end-members result in the breakdown of long-range order, a reduction in T_C, and the onset of relaxor behavior. As a general rule, increasing the number of cations in a solid solution tends to further undermine polar coherence and deepen the relaxor nature;[25] however, incorporation of $PbTiO_3$ in nano-polar systems tends to overcome the loss of coherence and favors the formation of long-range polar order. This can be clearly seen in the example of $BiFeO_3–PbTiO_3–(K_{0.5}Bi_{0.5})TiO_3$ in which the largest weak-field d_{33} is located virtually mid-way between the $BiFeO_3–PbTiO_3$ MPB composition and the pseudo-cubic region of $BiFeO_3–(K_{0.5}Bi_{0.5})TiO_3$.[26]

In order to address the problem of the $BiFeO_3$-$PbTiO_3$ system's high electrical conductivity and to prevent spontaneous sample destruction during the phase transition as a result of the substantial volume difference between the tetragonal and cubic phases, a third component $Li_{0.5}Bi_{0.5}TiO_3$, has been selected as the ternary component. With this approach, we do not introduce new elements at the B position, but only introduce aliovalent doping at the A position of the perovskite structure, which must locally compensate for electrical charges. Due to the large difference in the ionic radii of bismuth (lead) ions and lithium ion, doping with lithium-based titanate leads to reduced local stresses in the structure that will reduce the macroscopic stresses in the material in general. Lithium's ionic size and valence might make it particularly effective in forming or stabilizing oxygen vacancies in the lattice structure of the material. This should result in a more balanced and stable lattice structure, which in turn could reduce internal stresses. So, the introduction of lithium not only serves to reduce local stresses through ionic size considerations but also adds a chemical contribution that further stabilizes the lattice and thereby enhances the overall piezo-electrical properties of the material.

The main goal of this work was to study the effect of quenching and annealing on the piezoelectric properties of the most promising BFO ternary alloy of this latter type: $0.60BiFeO_3–0.25PbTiO_3–0.15Li_{0.5}Bi_{0.5}TiO_3$. The idea of rapid cooling is to maintain the randomized defect structure at the high temperature (above T_c) and to prevent (or control) the defect ordering on domain walls formed at temperatures below T_c. This concept has used to study hardening–softening transitions in PZT ceramics.[8] No detailed study of this transition in BFO-based ternary ceramics has been reported in the literature yet. The ability to reverse the quenching effect by a subsequent heat treatment has not been published previously. It will be shown to be an important aspect when studying the possibility of using this ceramic at elevated temperatures. The study of various heat treatments (such as quenching and annealing) for piezoelectric materials can open up new possibilities to tune their final properties. Such studies indirectly also deepen our understanding of the interaction of point defects and domain walls in ferroelectric materials.

II. EXPERIMENTAL PROCEDURE

$BiFeO_3–Bi_{0.5}Li_{0.5}TiO_3–PbTiO_3$ (BFO-BLT-PT) samples were prepared by a conventional solid-state reaction using analytical-grade commercially supplied raw materials: Bi_2O_3, Fe_2O_3, TiO_2,

PbO, and Li_2CO_3. Dried powders were weighed and ground separately before mixing. The $Bi_{0.5}Li_{0.5}TiO_3$ and $PbTiO_3$ levels were fixed at 0.15 and 0.25, respectively. Hence, the final composition can be written as $0.60BiFeO_3$–$0.25PbTiO_3$–$0.15Li_{0.5}Bi_{0.5}TiO_3$. Grinding and mixing processes were performed in isopropanol using yttria-stabilized ZrO_2 balls. The particle size distributions of the milled powder are in the range of 0.5–1 μm according to SEM images. Mixed powders after drying were calcined at 800 °C for 1 h using a heating rate of 600 °C/h. Then, the calcined powders were reground, granulated by mixing with 2 wt. % QPAC 40 binder, and uniaxially pressed into disks (13 mm in diameter and 1 mm in thickness) under 200–250 MPa. The pellets were sintered at 1025 °C for 1h using a heating and cooling rate of 600 °C/h. The sintering protocol is shown in detail in Fig. S1 of the supplementary material.

Scanning electron microscope (SEM) images were taken using a Jeol JSM-7500F field emission scanning electron microscope. Prior to SEM measurements, a thin (15 nm) layer of gold was deposited on the sample. To determine the phase purity, x-ray diffraction studies with Cu Kα radiation were done using a Bruker D8 Discover diffractometer. Scans were recorded at set temperatures: RT, 200°–700 °C in steps of 25 °C and again at RT after cooling down by switching off the heating. The density was determined by Archimedes' method in an aqueous medium.

Polarization–electric field hysteresis loops were measured at room temperature using a Radiant precision ferroelectric analyzer. The electrical properties of samples were measured at room temperature using an Agilent 4263B LCR meter at 1 kHz and 1 V. For these measurements, silver electrodes were applied on the ceramics by firing silver paste at 150 °C. For the actual research, electrode coated samples were thermally treated by gradual heating to a predetermined temperature of 600–750 °C, temperature stabilizing for 30 min, and then abrupt cooling in air or other media (silicone oil, ceramic plate, liquid nitrogen) to vary the cooling rate. Cooling rate variations were achieved in the range from 0.1 °C/s (furnace cooling) to 50–80 °C/s (metal contact). The conditions of quenching of the samples are shown in detail in Fig. S2 in the supplementary material. In this publication, the term "quenching temperature" refers to the temperature from which the sample was rapidly cooled to room temperature. Conversely, the "annealing temperature" refers to the temperature to which the sample was slowly heated, left to anneal for a specific period of time, and then gradually cooled down afterward.

After dielectric measurements, the samples were polarized under a DC electric field of 70 kV/cm for 20 min in silicone oil at room temperature. After aging for 24 at ambient laboratory conditions, the piezoelectric constant d_{33} was measured with a PM300 Berlincourt-type piezometer from Piezotest with a static force of 10 N and a dynamic force of 0.25 N peak to peak with sinusoidal excitation at 110 Hz. Samples were then annealed by placing them in a preheated furnace at temperature of 150–600 °C for a period of 7 min up to 2 weeks. After annealing and air cooling, the dielectric and piezoelectric parameters at room temperature were measured again.

III. RESULTS

A. Microstructure and crystal structure

Figure 1 shows the microstructure of a polished sample after chemical etching. The grain size is approximately 2–3 μm.
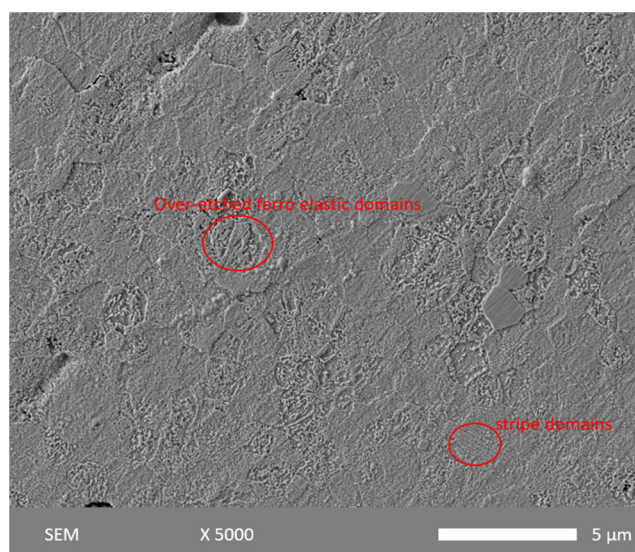

FIG. 1. SEM picture of a polished as-sintered sample after chemical etching. The encircled regions show the domain structure.

Ferroelectric and ferroelastic domain walls are partially visible, but the resolution is too small to properly show the domain size of 50–100 nm. The microstructure of the quenched and annealed samples does not differ from that of the as-sintered sample and are shown in the supplementary material Fig. S3 for the sake of completeness.

The XRD pattern is shown in Fig. 2 for three samples: (1) as-sintered which was oven cooled (i.e., cooling rate 0.05 °C/s from
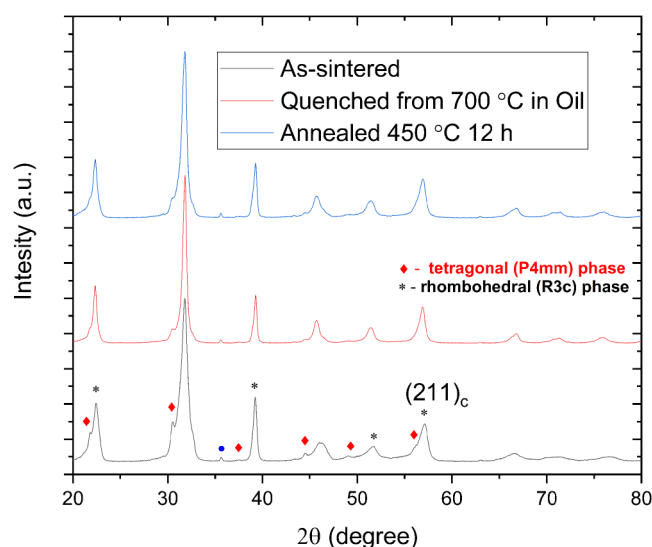

FIG. 2. X-ray diffraction patterns of the as-sintered, oil quenched from 700 °C and 12 h, 450 °C annealed after oil quenching samples.
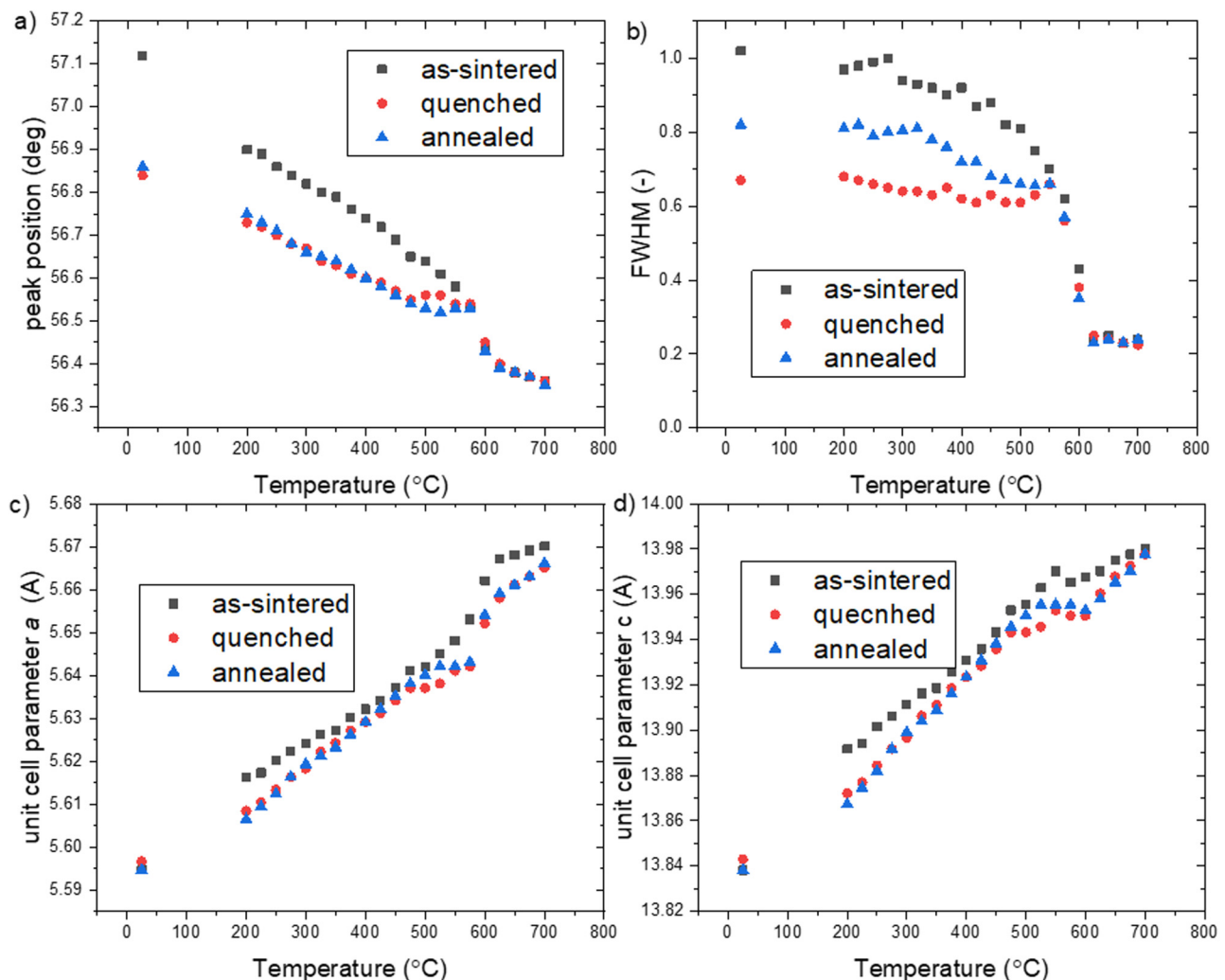
09 October 2023 11:49:05

700 °C, (2) oil quenched (i.e., cooling rate 60 °C/s from 700 °C, and (3) annealed for 12 h at 450 °C after oil quenching. The figure shows that two phases, rhombohedral and tetragonal, are coexisting (some non-overlapping peaks were marked on the figure). The diffraction peak at 37° (marked with the blue circle) is an artefact and is associated with the aluminum sample holder material. No peaks belonging to secondary phases were found indicating good solubility of all components and the formation of a solid solution. Upon annealing of the quenched sample, the peaks change in intensity, but no change in the peak position (i.e., the crystal structure) is observed.

B. Influence of temperature on the crystal structure

Figure 3 shows the evolution of the rhombohedral into the cubic phase as evidenced by the (associated) $(211)_C$ peak for the

same three sample conditions used in Fig. 2. This peak was chosen for the following reasons: a relatively high intensity while being located at a high angle, and no strong overlap with peaks of the tetragonal phase. Both the curves of the peak position and the average peak width indicate that the phase transition occurs over a temperature range of 600–625 °C. The peak position curves for the quenched and annealed samples show an unexpected plateau between 500 and 575 °C but are otherwise linear. The peak position curve of the as-sintered material only shows a linear temperature dependence up to the transformation temperature. Figure 3(a) also shows that the peak position changes markedly upon quenching, but that annealing has no effect on the peak position. This is in contrast with Fig. 3(b) which shows that the reduction of the peak position due to quenching is partially reverted by the annealing treatment. FWHM plotted after deconvolution of the recorded

FIG. 3. (a) Peak position; (b) full with at half maximum of (211) cubic reflection; (c) and (b) unit cell parameter a and c of R3c phase depending on the temperature for samples as-sintered, oil quenched from 700 °C and annealed 12 h at 450 °C.

peak. The unit cell parameter shown in Figs. 3(c) and 3(d) is almost identical for all three samples and also show a phase transition in the temperature range of 600–625 °C. The interpretation of the observed changes is discussed in Sec. IV.

C. The effect of the pre-quenching temperature on the ferroelectric properties

To study the minimal annealing temperature required to mobilize the defects, the P-E hysteresis loops were obtained for the as-sintered condition and for oil-quenched (silicon oil at room temperature) samples quenched from different temperatures. These P-E hysteresis loops are shown in Fig. 4. The well-saturated loops for samples quenched from temperatures from 650 to 750 °C demonstrate remnant polarization in the range of 20–25 $\mu C/cm^2$, but there is no visible trend in the change of the maximum and remnant polarization values depending on quenching temperature for this temperature range. But there is a clear trend in the reduction of the coercive field from 42 to 40 kV/cm with an increase in the quenching temperature from 650 to 750 °C. At quenching temperatures below 650 °C, we no longer observe saturated ferroelectric hysteresis loops. The transition temperature of around 625–650 °C is a bit higher than the transition temperature, 600–625 °C obtained from high temperature XRD data [Fig. 3]. The data indicate that during the phase transformation from a rhombohedral to cubic structure, the piezoelectric domains disappear, and that the reforming domain walls remained unpinned provided the cooling rate is high enough.

The P-E hysteresis loop obtained for the sample oil quenched from 700 °C and poled at 70 kV/cm for 20 min at room temperature is shown in Fig. 5, which exhibits a bias field (piezoelectric charge constant after poling reached 95 pC/N). This clearly indicates the presence of a sufficient number of defects that participate in polarization.[27] This result may indicate a hardening–softening transition similar to acceptor doped PZT.[8]
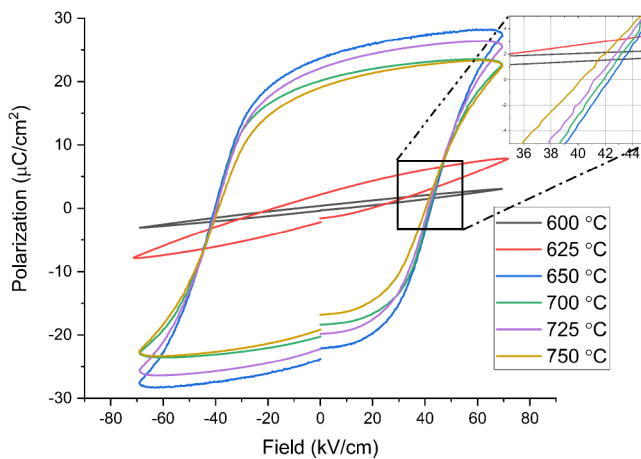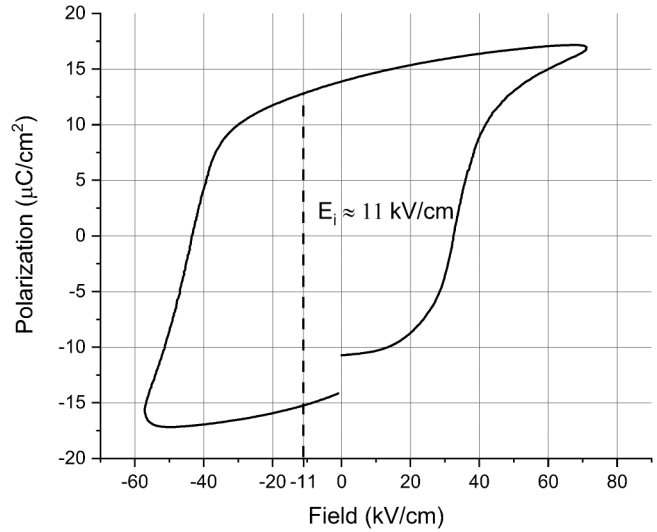

FIG. 5. Typical ferroelectric hysteresis loop after poling at 70 kV/cm for an oil quenched sample quenched from 700 °C.

For indirect determination of the transition temperature to the paraelectric state, the thermal depolarization of d_{33} was measured, and the results are shown in Fig. 6. It can be seen that both for the as-poled and for the annealed samples, a rapid depolarization occurs at a temperature above 600 °C and an approximate transition lies in the region of 625–650 °C. It can also be seen that for the as-poled sample, a smooth decrease in the piezoelectric constant d_{33} occurs at temperatures above 125–150 °C.

FIG. 4. Ferroelectric hysteresis of samples quenched from different temperatures in silicone oil.
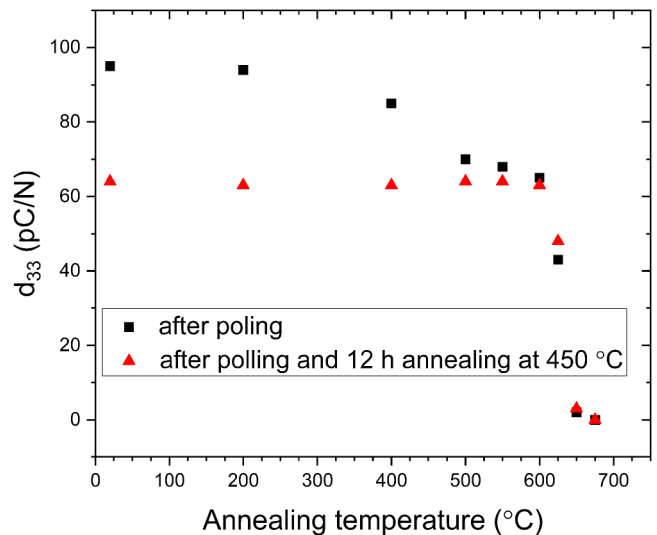

FIG. 6. Effect of thermal depolarization on d_{33} values of poled samples after poling and after annealing at 450 °C measured *ex situ* (at room temperature after heating up till target temperature for 15 min).

D. Effect of cooling rate during quenching from 700 °C on ferroelectric properties

In Fig. 7(a), the P-E loops up to 80 kV/cm are shown for various cooling rates from a fixed annealing temperature of 700 °C. The figure shows that for cooling rates higher than 10 °C/s, the P-E loops open up at a coercive field of about 50 kV/cm. At lower cooling rates, the P-E loops do not open up properly. As shown in Fig. 7(b), the remnant field strength shows an increase with increasing the cooling rate and the polarization for a cooling rate slower than 0.2 °C/s the ferroelectric loop will not differ from that for the as-sintered sample. Data do not allow draw conclusion on the dependence of remnant polarization on cooling rate. All measurements shown in Fig. 7 were successively performed on a single sample with the return of its original properties (as-sintered) upon annealing at 450 °C for 12 h.
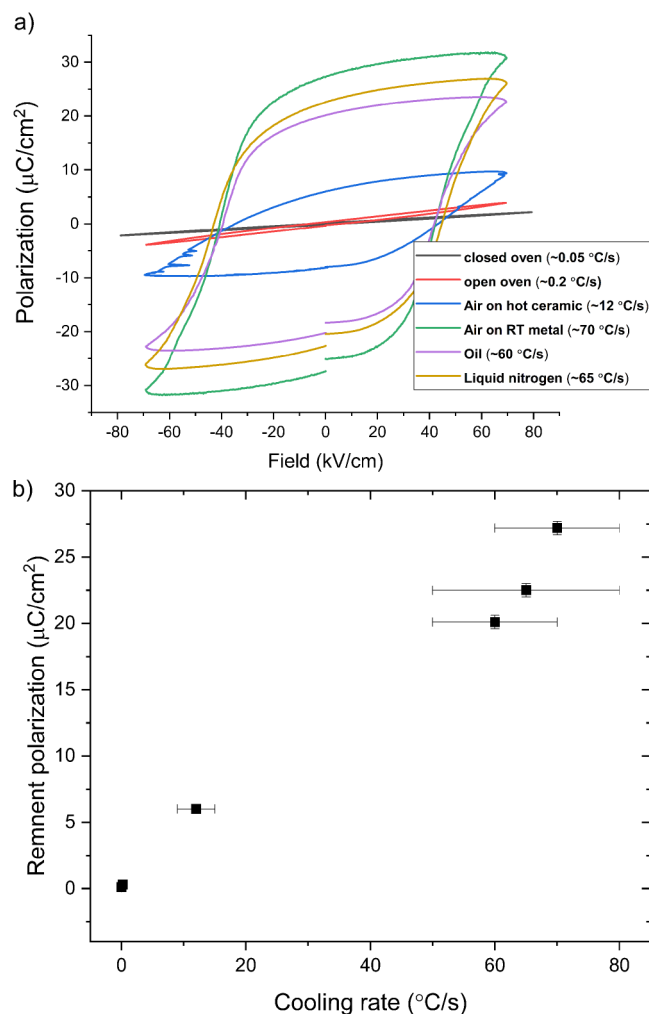
FIG. 7. (a) Ferroelectric hysteresis loops of a single sample quenched from 700 °C at different cooling rates, (b) remnant polarization as a function of the cooling rate.

E. Effect of post-quenching annealing on piezoelectric and electric properties

If the sample is quenched from 700 °C at a rate of around 50 °C/s and subsequently poled at a field of 70 kV/cm, the material is piezoelectrically activated and values of d_{33} of 95 pC/N (at room temperature) are achieved. Figure 8 shows the dynamics of changes in the (room temperature) piezoelectric and dielectric properties of optimally quenched samples upon subsequent isothermal annealing in air at different temperatures [(a) 150 °C, (b) 300 °C, (c) 450 °C, and (d) 600 °C]. We observe that a noticeable decrease in the piezo-electric property values occurs upon annealing at 300 °C or higher temperatures. Interestingly, the actual temperature does not affect the final value of the piezoelectric constant, which reaches a value of 63 pC/N, but only affects the kinetics of the change. All high temperature annealed samples eventually reach the same piezoelectric property value, which we consider to be the thermodynamically metastable state (intermedium) for our material.

Finally, we performed a number of successive annealing treatments at different temperatures to get a better insight into the apparent intermedium state leading to a d_{33} of 63 pC/N. To this aim, a sample was first annealed at 150 °C for times up to 20.160 min (i.e., 2 weeks), subsequently at 300 °C again for times up to 20 160 min (i.e., 2 weeks), and finally 2 weeks at 450 °C; and the piezo and dielectric properties were measured intermittently. The results are shown in Figs. 9(a)–9(c) for d_{33}, the dielectric constant and tan δ, respectively. The figure clearly shows that in the case of successive annealing the final values for d_{33} and the dielectric constant finally obtained, 63 pC/N and 225, respectively, are the same as those for the samples directly annealed at 450 °C, but that the total annealing time required was considerably longer. It should be especially noted that no matter what the temperature history of the sample, if the depolarization temperatures are not reached, the piezoelectric properties of the material will be in the region of 63 pC/N.

F. Repeatability of the quenching–annealing cycle

Figure 10 shows the results of measurements of ferroelectric hysteresis loops after multiple quenching cycles from 700 °C in oil and subsequent 12 h annealing at 450 °C at which conditions the piezoelectric properties should reach a plateau. It can be seen that the remnant polarization of the material decreases with each subsequent quenching cycle. The behavior is similar to that encountered in the fatigue phenomenon for piezoelectric materials (i.e., a repeated application of electric fields to the device leading to a lowering of the piezoelectric coefficients over time),[28] but in contrast to it, the original polarization value is not restored when the sample is re-annealed at a temperature above the Curie temperature.[29]

However, as can been seen from Fig. 11, the piezoelectric properties, unlike the remnant polarization, of the material practically do not change after multiple annealing and quenching cycles.

IV. DISCUSSION

A. Comparison of realized properties with those of other BFO systems

Recently, BFO-PT-based ternary solid solutions, such as BFO-PT-BT, BFO-PT-BZ, and BFO-PT-BZT, other than the
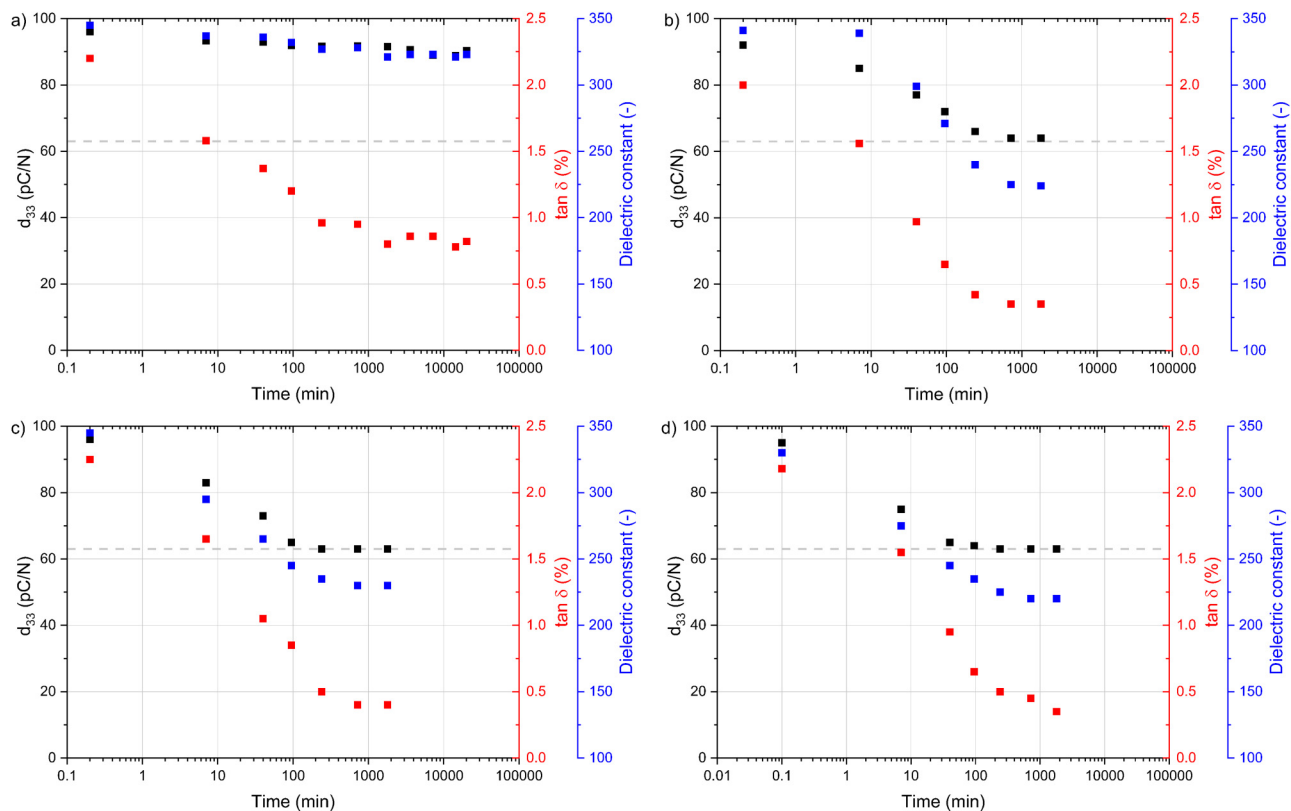
FIG. 8. Effect of post annealing at (a) 150 °C and (b) 300 °C on piezoelectric and dielectric properties of sample. Symbol color corresponds to the color of the parameter mentioned on the Y axes. Dashed line shows the stable value of piezoelectric constant at 63 pC/N. Effect of post annealing at (c) 450 °C and (d) 600 °C on piezoelectric and dielectric properties of the sample. Symbol color corresponds to the color of the parameter mentioned on the Y axes. Dashed line shows the stable value of piezoelectric constant at 63 pC/N.

current ternary system investigated here, have attracted much attention. The published studies showed high piezoelectric properties up to 300–400 pC/N (at room temperature).[30–33] However, these piezoceramics generally have a high coercive field up to 60–100 kV/cm, which creates difficulties in fully activating the piezoelectric properties upon poling. But, they certainly outperform the studied in this work system with a coefficient of 65 pC/N in terms of raw piezoelectric performance.

However, the Curie temperature of these reported BFO-based systems is between 200 and 300 °C, indicating a notable limitation in terms of thermal stability in comparison to our system which can be made stable up to 600 °C. Thus, while offering stronger piezoelectric responses at room temperature, the operational window in terms of temperature of published ternary BFO systems is significantly lower than that of the system presented here.

To put the performance of the current material in an even wider perspective, traditional PZT (lead zirconate titanate) exhibits piezoelectric coefficients typically ranging between 200 and 400 pC/N and demonstrates stability up to its Curie temperature, around 100–250 °C.[34] Quartz, another well-known material, has a coefficient of about 2.3 pC/N and can maintain its properties up to

approximately 573 °C.[35] LiNbO₃ (lithium niobate) can achieve coefficients between 60 and 130 pC/N and has a general stability nearing 1250 °C, though its piezoelectric properties might degrade before this point.[35] Lastly, ZnO (zinc oxide) presents a coefficient of approximately 12 pC/N and can withstand temperatures up to 1975 °C, even though its piezoelectric properties may degrade prior to reaching this temperature.[36] So, our proposed system offers a good balance of piezoelectric properties and high temperature stability, even if other systems may perform better in only one of these aspects.

B. "Quenching" effect mechanism

The primary explanation of quenching may be the transformation of ferroelectric domains during cooling into a certain quasi-stable state, not associated with surrounding defects.[8] Based on the fact that the cooling rate should exceed a certain value (higher than 10 °C/s) to open ferroelectric loops as shown in Fig. 7(b), it can be assumed that defects that are free at high temperatures, have a limited lifetime before they take a more thermodynamically stable position near the domain walls. The transition from a closed

09 October 2023 11:49:05
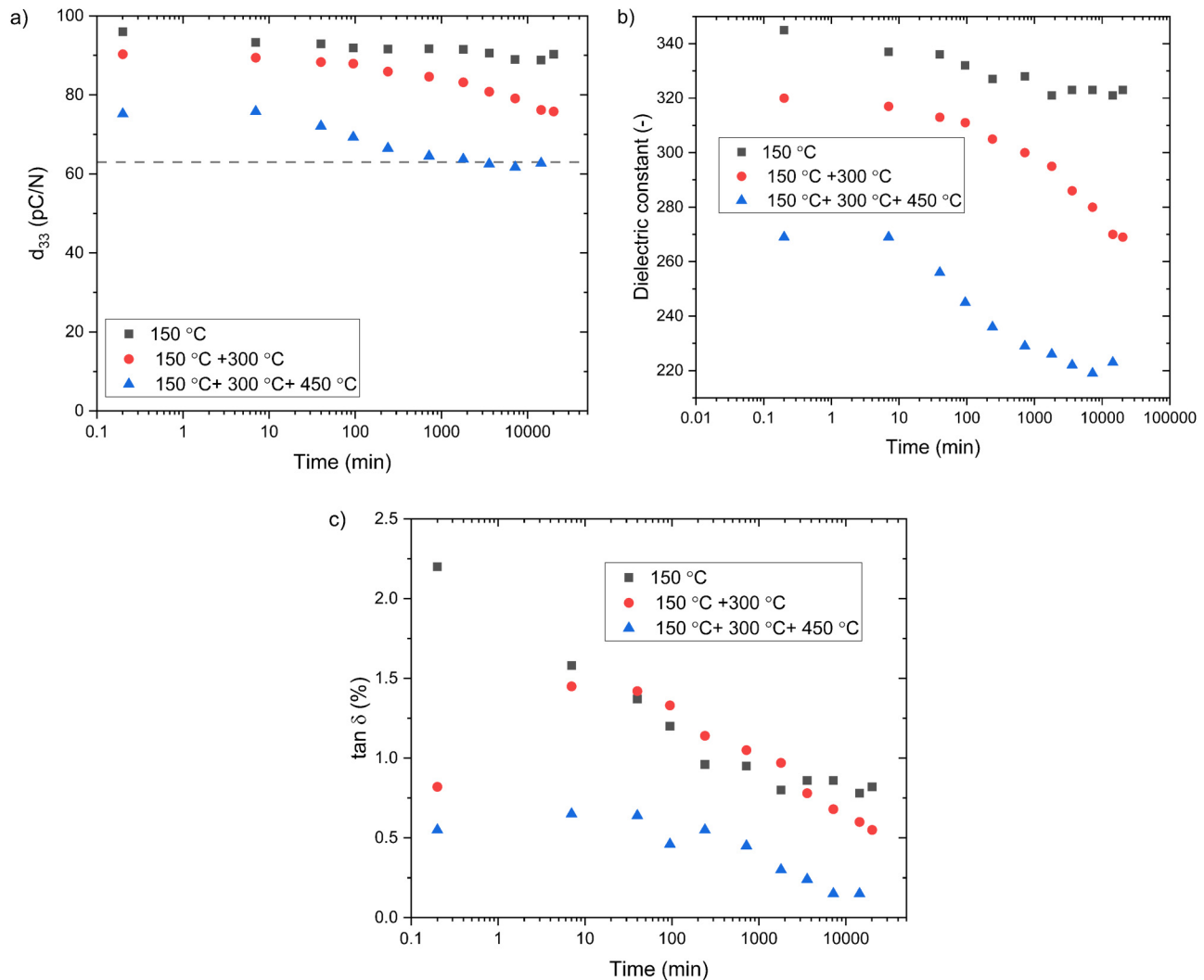
FIG. 9. (a) Piezoelectric charge constant (dashed line shows the stable value of piezoelectric constant at 63 pC/N) and (b) dielectric constant of the quenched sample depending on the total time at annealing temperatures of 150 °C, 150 + 300, and 150 °C + 300 °C + 450 °C (detailed thermal history shown in Fig. 4S), (c) dielectric losses of quenched sample depending on the total time at annealing temperatures of 150 °C, 150 + 300, and 150 °C + 300 °C + 450 °C (detailed thermal history shown in Fig. 4S).

ferroelectric hysteresis loop to an open loop occurs only upon quenching from a temperature of 650 °C and higher, so it can be assumed that the phase transition from the ferroelectric state to the para-electric state plays an important role in the formation of this effect.[11,37] It is shown indirectly by the thermal depolarization curve of d_{33} that all the piezoelectric properties of the material disappear when heated above 650 °C as a result of the phase transition in materials [Fig. 6]. It should be remembered that the actual *in situ* high temperature XRD data show that the phase transition does occur at a slightly lower temperature (600–625 °C). We have no real physical explanation for the observed temperature difference and blame it on instrumental issues. But it is also worth

noting that there is no noticeable change in the crystallographic structure of the samples directly after quenching from 700 °C and after subsequent annealing at 450 °C while the difference in piezo-electric behavior is extreme. Only for the sintered sample a slight phase shift of the (211) peak is observed at room temperature. As shown in Fig. 3(b), all samples achieve a similar full width at half maximum at high temperature, which indicates a diffusive phase transition at temperatures above 600 °C, which correlates well with the presence of a minimally required quenching temperature, while the width depends on the temperature history of the sample. The synthesized sample has the largest peak width at room temperature, and the quenched sample has the smallest. While the width of the
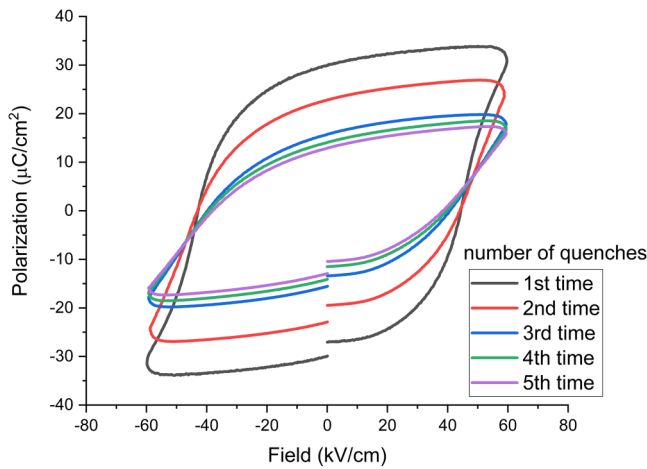
09 October 2023 11:49:05

FIG. 10. P-E loops after multiple cycles of quenching from 700 °C in oil with subsequent 12 h annealing in air at 450 °C.

FIG. 12. d_{33} values of poled samples depend on annealing temperature.[39]

peak may be responsible for the internal stresses accumulated in the ceramic, it is not typical to have a lower stress in the quenched samples.[38]

C. Annealing after quenching

During subsequent annealing, two potentially competing processes may occur. One of which is the reorientation of unstable domains, and the second is the diffusion of defects to the domain walls, which, as a result, bind them. This may explain the decrease in the piezoelectric response upon subsequent annealing to a
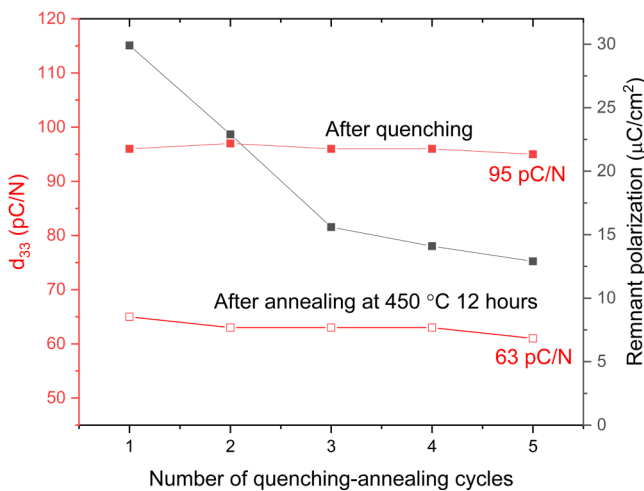

FIG. 11. Piezoelectric and ferroelectric properties after multiple quenching–annealing cycles. Symbol colors correspond to the label colors on the X and Y axes.
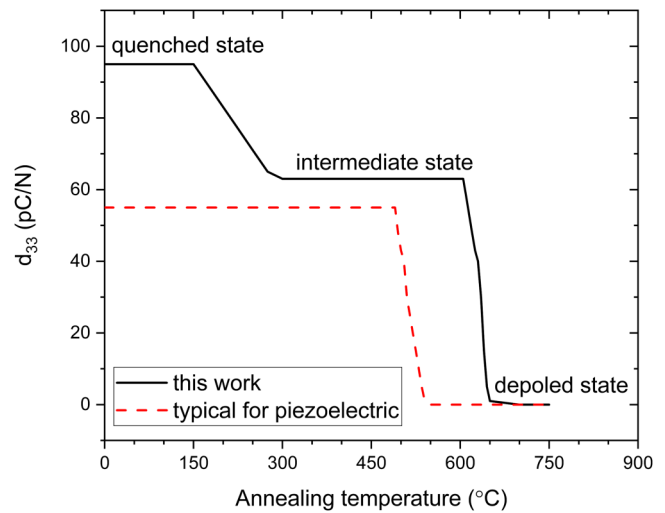
certain stable value. But it cannot explain the fact that the piezoelectric constant value at the intermediate state does not depend on the annealing temperature. Another assumption is that the change in the piezoelectric properties may be caused by a change in the dielectric constant of the material during annealing due to the binding of mobile charges. Since the piezoelectric constant is directly proportional not only to the polarizability but also to the dielectric constant, then, at a constant polarizability and with a decrease in the permeability, the piezoelectric constant of the material can be reduced.[35] Contrary to this expected correlation, it was noticed [Fig. 8(a)] that a decrease in dielectric losses occurs also upon low-temperature annealing while the piezoelectric constant remains more or less constant. High dielectric losses after quenching are presumably associated with the generation of free charge carriers, which, upon subsequent annealing, form dipole complexes or recombine.[17] Therefore, it can be assumed that annealing mainly affects free charge carriers and not bound dipoles.

Figure 6 shows the thermal depolarization curves obtained in our work. The main difference between results obtained in our work and the usual published depolarization curves for piezoelectric ceramics[39] is that after annealing above a certain temperature (100–150 °C), the samples transform into an intermediate state, which is characterized by a lower yet significant value for the piezoelectric constant [Fig. 12]. This is different from depolarization curves for conventional piezo ceramics, for which the value decreases to zero during long enough annealing.

So during annealing, the quenched state of the more mobile domain walls and point defects is destroyed, and the material pass into an intermediate state, in which the coercive field is much larger. Therefore, poling of the samples is possible only in the quenched state, because in annealed states, the material's characteristics will prevent successful polarization without compromising the mechanical integrity of the sample (leading to dielectric breakdown and sample disintegration). The value of the piezoelectric

charge constant of samples in the intermediate state does not depend on the annealing temperature as shown in Fig. 7. An increase of the annealing temperature, as long as the depolarization temperature is not exceeded, only accelerates the process to reach this state.

D. Reversibility of the quenching-annealing

As shown in Sec. IIIF, the effect of quenching and annealing can be reversed. Re-quenching of re-annealed samples fully restores the quenched state, while subsequent annealing brings the sample to an intermediate state again. These cyclic changes in both electrical and piezoelectric parameters indirectly indicate a change in the mobility of domain walls and point defects. The absence of a change in the piezoelectric parameters in cycles shows the complete reversibility of this transition. Based on the reversibility of the quenching, we can assume that it is associated with defects and a similar hardening mechanism as that which occurs in acceptor-doped PZT,[40] is involved. The mechanism of precipitation hardening[41] as a result of the formation of secondary phases can be considered as being unlikely due to the fact that no secondary phases after quenching could be detected in XRD. The effect of fatigue of ceramics during repeated reproduction of the effect cannot be directly explained by defects and phase transition and can be caused by microcracks arising from aggressive impact on ceramics.

V. CONCLUSIONS

Piezoelectric properties of $BiFeO_3$–$Bi_{0.5}Li_{0.5}TiO_3$–$PbTiO_3$ ceramic can be changed by thermal processing. Good properties at room temperature can be obtained by sufficiently fast cooling from temperature above phase transition temperature (T > 650 °C). The cooling rate is essential in this process and must be above a certain threshold (in our study, above 10 °C/s).

The non-equilibrium state can be mediated by proper annealing, shifting material to an unusual but clearly identifiable intermediate state. The transition to intermediate state occurs spontaneously at annealing temperatures above 150 °C. An increase in annealing temperature leads to an acceleration of this transition but not to a change in final properties. For this ternary system, it is possible to distinguish three states obtained for this material: quenched (full polarization), intermediate, and depoled, while for common piezoceramics, there is only a poled and depoled state. Thermal depolarization takes place when annealing at T > 650 °C

Although the nature of this effect is not fully understood, all observed changes can be attributed to defect reorganization. The nature of the defects has not been investigated here. Our assumption is that this effect is related to the uniform distribution of point defects over the sample during quenching and the subsequent movement of these defects to domain walls that connect them during tempering. This is supported by the fact that this effect is completely reversible, if we properly reheat and adequately quench the ceramic again, we will release the domains and we can bind them again when annealed. For further research, it would be useful to find another mechanism for controlling the distribution of defects and study the processes on the domain walls *in situ*.

AUTHOR DECLARATIONS

Conflict of Interest

The authors have no conflicts to disclose.

Author Contributions

Anton Tuluk: Conceptualization (lead); Investigation (lead); Methodology (equal); Writing – original draft (lead); Writing – review & editing (equal). **Sybrand van der Zwaag:** Supervision (lead); Writing – review & editing (equal).

DATA AVAILABILITY

The data that support the findings of this study are available from the corresponding author upon reasonable request.

REFERENCES

[1] J. Seidel, L. W. Martin, Q. He, Q. Zhan, Y. H. Chu, A. Rother, M. E. Hawkridge, P. Maksymovych, P. Yu, M. Gajek, N. Balke, S. V. Kalinin, S. Gemming, F. Wang, G. Catalan, J. F. Scott, N. A. Spaldin, J. Orenstein, and R. Ramesh, Nat. Mater. **8**, 229 (2009).

[2] T. Rojac, A. Bencan, G. Drazic, N. Sakamoto, H. Ursic, B. Jancar, G. Tavcar, M. Makarovic, J. Walker, B. Malic, and D. Damjanovic, Nat. Mater. **16**, 322 (2017).

[3] A. N. Morozovska, R. K. Vasudevan, P. Maksymovych, S. V. Kalinin, and E. A. Eliseev, Phys. Rev. B: Condens. Matter Mater. Phys. **86**, 1 (2012).

[4] U. Robels and G. Arlt, J. Appl. Phys. **73**, 3454 (1993).

[5] X. Ren, Nat. Mater. **3**, 91 (2004).

[6] R. A. Eichel, Phys. Chem. Chem. Phys. **13**, 368 (2011).

[7] M. I. Morozov, M. A. Einarsrud, J. R. Tolchard, P. T. Geiger, K. G. Webber, D. Damjanovic, and T. Grande, J. Appl. Phys. **118**, 164104 (2015).

[8] M. I. Morozov and D. Damjanovic, J. Appl. Phys. **104**, 034107 (2008).

[9] N. Horchidan, C. E. Ciomaga, R. C. Frunza, C. Capiani, C. Galassi, and L. Mitoseriu, Ceram. Int. **42**, 9125 (2016).

[10] T. Rojac, A. Bencan, B. Malic, G. Tutuncu, J. L. Jones, J. E. Daniels, and D. Damjanovic, J. Am. Ceram. Soc. **97**, 1993 (2014).

[11] J. Lv, X. Lou, and J. Wu, J. Mater. Chem. C **4**, 6140 (2016).

[12] I. Calisir, A. A. Amirov, A. K. Kleppe, and D. A. Hall, J. Mater. Chem. A **6**, 5378 (2018).

[13] S. Lee, C. A. Randall, and Z. K. Liu, J. Am. Ceram. Soc. **90**, 2589 (2007).

[14] J. M. Vitek, A. Dasgupta, and S. A. David, Metall. Trans. A: Phys. Metall. Mater. Sci. **14A**, 1833 (1983).

09 October 2023 11:49:05

[15]W. Deng, D. Zhang, H. Wu, Z. Huang, K. Zhou, and L. Jiang, Scr. Mater. **183**, 139 (2020).

[16]T. K. Gupta, J. Am. Ceram. Soc. **55**, 249 (1972).

[17]K. V. Lalitha, B. Wang, P. Ren, D. A. Hall, and T. Rojac, Open Ceram. **10**, 100259 (2022).

[18]M. Čebela, D. Zagorac, K. Batalović, J. Radaković, B. Stojadinović, V. Spasojević, and R. Hercigonja, Ceram. Int. **43**, 1256 (2017).

[19]G. L. Yuan, S. W. Or, Y. P. Wang, Z. G. Liu, and J. M. Liu, Solid State Commun. **138**, 76 (2006).

[20]Y. P. Wang, L. Zhou, M. F. Zhang, X. Y. Chen, J.-M. Liu, and Z. G. Liu, Appl. Phys. Lett. **84**, 1731 (2004).

[21]T. Rojac, M. Kosec, B. Budic, N. Setter, and D. Damjanovic, J. Appl. Phys. **108**, 074107 (2010).

[22]A. Bencan, G. Drazic, H. Ursic, M. Makarovic, M. Komelj, and T. Rojac, Nat. Commun. **11**, 1 (2020).

[23]B. Wang, Y. Li, and D. A. Hall, J. Am. Ceram. Soc. **105**, 1265 (2022).

[24]M. Ahart, M. Somayazulu, R. E. Cohen, P. Ganesh, P. Dera, H. K. Mao, R. J. Hemley, Y. Ren, P. Liermann, and Z. Wu, Nature **451**, 545 (2008).

[25]T. Sebastian, I. Sterianou, D. C. Sinclair, A. J. Bell, D. A. Hall, and I. M. Reaney, J. Electroceramics **25**, 130 (2010).

[26]A. J. Bell, T. P. Comyn, and T. J. Stevenson, APL Mater. **9**, 010901 (2021).

[27]S. Takahashi, Ferroelectrics **41**, 143 (1982).

[28]L. Zhang and X. Ren, Phys. Rev. B **73**, 094121 (2006).

[29]Y. A. Genenko, J. Glaum, M. J. Hoffmann, and K. Albe, Mater. Sci. Eng. B Solid-State Mater. Adv. Technol. **192**, 52 (2015).

[30]M. M. Kumar, A. Srinivas, and S. V. Suryanarayana, J. Appl. Phys. **87**, 855 (2000).

[31]C. Feng, Y. yun Feng, M. jia Fan, C. hui Geng, X. juan Lin, C. hong Yang, and S. feng Huang, J. Cent. South Univ **28**, 3747 (2021).

[32]Q. Li, Y. Dong, J. Cheng, J. Chen, and J. Mater, Sci. Mater. Electron. **27**, 7100 (2016).

[33]Y. Huang, L. Zhang, R. Jing, Y. Yang, V. Shur, X. Wei, and L. Jin, J. Mater. Sci. Technol. **169**, 172 (2024).

[34]P. M. Weaver, T. Stevenson, T. Quast, G. Bartl, T. Schmitz-Kempen, P. Woolliams, A. Blumfield, M. Stewart, and M. G. Cain, J. Mater. Sci. Mater. Electron. **26**, 9268 (2015).

[35]S. Zhang and F. Yu, J. Am. Ceram. Soc. **94**, 3153 (2011).

[36]K. S. Srikanth, A. Wazeer, P. Mathiyalagan, S. Vidya, K. Rajput, and H. S. Kushwaha, *Piezoelectric Properties of ZnO* (Elsevier, 2021).

[37]H. C. Thong, Z. Li, J. T. Lu, C. B. W. Li, Y. X. Liu, Q. Sun, Z. Fu, Y. Wei, and K. Wang, Adv. Sci. **9**, 2200998 (2022).

[38]Y. Takagi, H. Nagata, and T. Takenaka, J. Asian Ceram. Soc. **8**, 277 (2020).

[39]T. L. Zhao, A. A. Bokov, J. Wu, H. Wang, C. M. Wang, Y. Yu, C. L. Wang, K. Zeng, Z. G. Ye, and S. Dong, Adv. Funct. Mater. **29**, 1807920 (2019).

[40]M. I. Morozov and D. Damjanovic, J. Appl. Phys. **107**, 034106 (2010).

[41]C. Zhao, S. Gao, T. Yang, M. Scherer, J. Schultheiß, D. Meier, X. Tan, H. J. Kleebe, L. Q. Chen, J. Koruza, and J. Rödel, Adv. Mater. **33**, 2102421 (2021).

09 October 2023 11:49:05